

Effective Edge Centrality via Neighborhood-based Optimization

Renchi Yang

Department of Computer Science
Hong Kong Baptist University
renchi@hkbu.edu.hk

Abstract

Given a network G , *edge centrality* is a metric used to evaluate the importance of edges in G , which is a key concept in analyzing networks and finds vast applications involving edge ranking. In spite of a wealth of research on devising edge centrality measures, they incur either prohibitively high computation costs or varied deficiencies that lead to sub-optimal ranking quality.

To overcome their limitations, this paper proposes ECHO, a new centrality measure for edge ranking that is formulated based on neighborhood-based optimization objectives. We provide in-depth theoretical analyses to unveil the mathematical definitions and intuitive interpretations of the proposed ECHO measure from diverse aspects. Based thereon, we present three linear-complexity algorithms for ECHO estimation with non-trivial theoretical accuracy guarantees for centrality values. Extensive experiments comparing ECHO against six existing edge centrality metrics in graph analytics tasks on real networks showcase that ECHO offers superior practical effectiveness while offering high computation efficiency.

1 Introduction

Edge centrality is a fundamental tool in network analysis for assessing the importance of edges within a network G , which empowers us to rank edges in terms of both network topology and dynamics (White and Smyth 2003). In the past decades, edge centrality has seen widespread use in a variety of applications, such as identifying strong ties in social networks (Ding et al. 2011), protection of infrastructure networks (Bienstock, Chertkov, and Harnett 2014), identification of failure locations in materials (Pournajar, Zaiser, and Moretti 2022), community detection (Fortunato, Latora, and Marchiori 2004), transportation (Jana et al. 2023; Crucitti, Latora, and Porta 2006), and many others (Mitchell, Agrawal, and Parker 2019; Yoon, Blumer, and Lee 2006; Cuzzocrea et al. 2012; Wang et al. 2023; Lai et al. 2024).

In the literature, extensive efforts have been devoted towards designing effective centrality metrics for edge ranking (Bröhl and Lehnertz 2019; Kucharczuk, Was, and Skibski 2022). As reviewed in Section 2, the majority of them can be classified into three categories: *ratio-based*, *recursive-based*, and *leave-one-out* centrality measures, as per their definitional styles. The ratio-based scheme conceives of edge importance as the fraction of sub-structures in the input network G embodying the edge. Two representatives include the

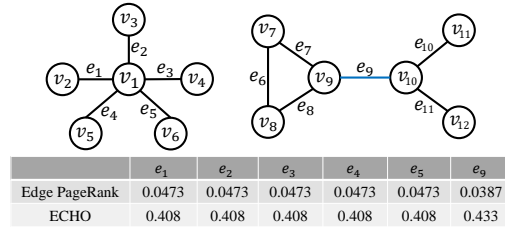


Figure 1: An example network G

well-known *edge betweenness* (Girvan and Newman 2002) and *effective resistance* (Spielman and Srivastava 2008), both of which entail tremendous computation overhead due to the enumeration of the shortest paths between all possible node pairs and minimum spanning trees in G . The leave-one-out centrality indices also suffer from severe efficiency issues, as they require calculating expensive network metrics by excluding each edge, causing a cubic time complexity. Moreover, these centrality metrics fail to account for directions of edges, and thus, produce compromised ranking effectiveness on directed networks.

To mitigate the foregoing issues, recent works extend prominent recursive-based centrality measures for nodes (e.g., PageRank (Page et al. 1998)) to their edge counterparts (e.g., edge PageRank), which enable us to compute the centralities of all edges in G with linear asymptotic complexity and cope with edge directions. Unfortunately, as pinpointed in Section 2, these metrics have inherent drawbacks as they quantify the edge importance merely using the strength of directed topological connections to one of its endpoints. As a consequence, such measures strongly rely on the assumption that G is connected, as the amount and strength of connections of nodes in various components in disconnected networks are incomparable. For instance, on the disconnected network with two components illustrated in Fig. 1, edge e_9 is intuitively more important to G than e_1 - e_5 as the deletion of it renders nodes v_7 - v_9 disconnected from nodes v_{12} - v_{12} , significantly altering the structure of G . However, if we adopt edge PageRank (EP) for edge ranking, the EP of e_9 (i.e., 0.0387) is much smaller than those of edges e_1 - e_5 (i.e., 0.0473), indicating that edges e_1 - e_5 are more valuable to G than e_9 and contradicting the above intuition. In summary, existing centrality measures for edges are either computationally demanding or suffer from limited ranking efficacy.

Furthermore, despite considerable research (Kucharczuk,

Was, and Skibski 2022; Murai and Yoshida 2019; Bao, Xu, and Zhang 2022) invested in theoretical analysis of these edge centrality metrics, to our knowledge, none of the extant studies have explored their practical effectiveness in downstream graph analytics tasks. Therefore, it still remains unclear which edge centrality metrics should be adopted in real applications.

In this paper, we propose a new centrality measure ECHO (Edge Centrality via neighborhood-based Optimization) for edge ranking in undirected or directed networks. More specifically, ECHO is formulated based on two neighborhood-based optimization objectives, where the former incorporates out-degrees of both endpoints of edges into the centrality values, while the latter forces the centrality scores of adjacent edges close. Such optimization goals require no assumptions on the network structure, i.e., connected or disconnected, and hence, enjoy better ranking effectiveness. For instance, if we revisit the example in Fig. 1, the issue of edge PageRank is now resolved when ECHO is utilized ($0.433 > 0.408$). Theoretically, to facilitate the intuitive understanding of ECHO, thorough theoretical discussions of ECHO from three perspectives are provided. Building on these interpretations, we further present three approximate algorithms for ECHO computation that run in time linear to the size of G , followed by theoretical analyses in terms of their approximation accuracy guarantees, time complexities, or convergence. Empirically, we demonstrate the superiority of ECHO over existing edge centrality measures in practical effectiveness through extensive experiments on six real datasets in three popular network tasks involving graph clustering, network embedding, and graph neural networks.

2 Preliminaries

2.1 Notations and Terminology

Throughout this paper, sets are symbolized by calligraphic letters, e.g., V , and $|V|$ is used to denote the cardinality of the set V . Matrices (resp. vectors) are represented as bold uppercase (resp. lowercase) letters, e.g., \mathbf{A} (resp. \mathbf{x}). We use superscript \mathbf{A}^\top to represent the transpose of matrix \mathbf{A} . $\mathbf{A}[i, j]$ denotes the (i, j) -th entry in matrix \mathbf{A} .

Let $G = (V, E)$ be a network (a.k.a. graph) with a node set V containing n nodes and an edge set E consisting of m edges. For each node $v \in V$, we denote by $N^-(v)$ (resp. $N^+(v)$) the set of incoming (resp. outgoing) neighbors of v . Particularly, $N^-(v) = N^+(v)$ when G is undirected. We use the diagonal matrix \mathbf{D} to represent the out-degree matrix of G , where each diagonal element $\mathbf{D}[v, v] = |N^+(v)|$. The adjacency matrix of G is symbolized by \mathbf{A} , in which $\mathbf{A}[u, v] = 1$ if $(u, v) \in E$, otherwise 0. The incidence matrix of G is denoted by $\mathbf{E} \in \mathbb{R}^{n \times m}$, wherein $\mathbf{E}[v_i, e_i] = 1$ if node v_i is incident with edge e_i , and $\mathbf{E}[v_i, e_i] = 0$ otherwise.

2.2 Existing Edge Centrality Measures

In what follows, we categorize existing edge centrality metrics into four groups and review each of them.

Ratio-based Edge Centralities. At a high level, this category of centralities utilizes the fraction of paths or spanning trees containing target edge $e = (u, v)$ to quantify

the importance of e in the network G . Amid them, *edge betweenness* (EB) (Girvan and Newman 2002) is one of the most classic measures, which is formally defined by $C_{\text{EB}}(e) = \sum_{s \neq t \in V} \frac{\delta_{s,t}(e)}{\delta_{s,t}}$, where $\delta_{s,t}$ signifies the number of shortest paths from s to t and $\delta_{s,t}(e)$ is the number of such paths passing through edge e . However, EB falls short of considering arbitrary paths that embody rich topological information (Stephenson and Zelen 1989). As a remedy, in (De Meo et al. 2012), the authors extend the κ -path centrality (Alahakoon et al. 2011) for nodes to edges, dubbed as *κ -path edge centrality* (KPC). More precisely, KPC $C_{\text{KPC}}(e)$ is the sum of the factions $\frac{\delta_s(e)}{\delta_s}$ of length- κ paths originating from every node $s \in V$ traversing edge e : $C_{\text{KPC}}(e) = \sum_{s \in V} \frac{\delta_s((u,v))}{\delta_s}$.

In lieu of using paths as in EB and KPC, *effective resistance* (ER) (Lovász 1993; Yang and Tang 2023) (a.k.a. *spanning edge betweenness/centrality* (Teixeira et al. 2013; Zhang et al. 2023) or *resistance distance*) relies on *minimum spanning trees* (MSTs). Formally, the ER of edge $e = (u, v)$ is formulated as $C_{\text{ER}}(e) = \frac{\tau_G(e)}{\tau_G}$, where τ_G is the number of distinct MSTs from G and $\tau_G(e)$ represents the number of distinct MSTs from G where edge e occurs. According to (Spielman and Srivastava 2008), the above mathematical definition can be equivalently rewritten as: $C_{\text{ER}}(e) = \mathbf{L}^\dagger[u, u] + \mathbf{L}^\dagger[v, v] - 2\mathbf{L}^\dagger[u, v]$, where \mathbf{L}^\dagger denotes the Moore-Penrose pseudo-inverse of the Laplacian (i.e., $\mathbf{L} = \mathbf{D} - \mathbf{A}$) of G . (Yi et al. 2018) pinpoints that ER fails to distinguish any pair of cut edges, and then based on (Lipman, Rustamov, and Funkhouser 2010) proposes a variant of ER, i.e., *biharmonic distance related centrality* (BDRC) in $C_{\text{BDRC}}(e) = \mathbf{L}^{\dagger^2}[u, u] + \mathbf{L}^{\dagger^2}[v, v] - 2\mathbf{L}^{\dagger^2}[u, v]$ as a remedy.

Recursive-based Edge Centralities. Another line of research resorts to a recursive definition. That is, the influence of an edge $e = (u, v)$ is proportional to the sum of the influence scores of other edges incoming to its starting point u . In the spirit of such an idea, (Chapela et al. 2015) extends prominent node-wise centrality measure PageRank (Page et al. 1998) to *edge PageRank* (EP) in Eq. (1), where the EP of edge $e = (u, v)$ is contributed by the EP values of all edges incident to the start node u and its self-importance. The parameter $\alpha \in (0, 1)$ is used to control the importance of the influence from such incoming edges.

$$C_{\text{EP}}(e) = \frac{1}{|N^+(u)|} \left(\alpha \sum_{x \in N^-(u)} C_{\text{EP}}((x, u)) + 1 \right) \quad (1)$$

Akin to EP, (Chapela et al. 2015) further extends *Katz index* (Katz 1953) to *Edge Katz* (EK) as follows: $C_{\text{EK}}(e) = \alpha \sum_{x \in N^-(u)} C_{\text{EK}}((x, u)) + 1$, (Huang and Huang 2019) extends *eigencentrality* for nodes (Bonacich 1972) to *Eigenedge* (EE), which can be regarded as a variant of EK.

Leave-One-Out Edge Centralities. In this category, the importance of an edge $e = (u, v)$ is evaluated by the change after excluding e from G in terms of a network metric. For example, the *information centrality* (IC) (Fortunato, Latora, and Marchiori 2004) of e is defined as the relative loss in the *network efficiency* obtained by removing $e = (u, v)$ from G : $C_{\text{IC}}(e) = \frac{\epsilon(G) - \epsilon(G \setminus e)}{\epsilon(G)}$, where $\epsilon(G)$ connotes the average

Table 1: Existing Edge Centralities

Centrality	Edge Direction	Complexity
Edge Betweenness (EB) (Girvan and Newman 2002)	✓	$O(n^2 + mn)$
κ -Path Edge Centrality (KPC) (De Meo et al. 2012)	✓	$O(m + n^2 \kappa)$
Effective Resistance (ER) (Spielman and Srivastava 2008)	✗	$O(mn^{\frac{3}{2}})$
BDRC (Yi et al. 2018)	✗	$O(m + n^3)$
Edge PageRank (EP) (Chapela et al. 2015)	✓	$O(m \log n)$
Edge Katz (EK) (Chapela et al. 2015)	✓	$O(m \log n)$
Eigenedge (EE) (Huang and Huang 2019)	✓	$O(m \log n)$
Information Centrality (IC) (Fortunato, Latora, and Marchiori 2004)	✓	$O(mn^2 \log n)$
θ -Kirchhoff Edge Centrality (θ -KEC) (Li and Zhang 2018)	✗	$O(mn^3)$
Kemeny Edge Centrality (KEC) (Altafini et al. 2023)	✗	$O(m^2 n)$
GTOM (Yip and Horvath 2007)	✓	$O(m \cdot \max_{v \in V} N^+(v))$
Current-Flow Centrality (CFC) (Brandes and Fleischer 2005)	✓	$O(mn \log n)$
Our ECHO	✓	$O(m \log m)$

network efficiency (i.e., the reciprocal of the distance of two nodes) (Latora and Marchiori 2001) of G . In analogy to IC, θ -Kirchhoff edge centrality (θ -KEC) of edge e is defined as the Kirchhoff index of the network obtained from G by deleting e (Li and Zhang 2018), where the Kirchhoff index of a network is the sum of effective resistances of all node pairs. Very recently, (Altafini et al. 2023) propose *Kemeny-based Edge Centrality* (KEC): $C_{\text{KEC}}(e) = K(G \setminus e) - K(G)$, where $K(G)$ represents the Kemeny’s constant (Kemeny and Snell 1960) of G , i.e., the expected number of time steps needed from a starting node u to a random destination node v sampled from the stationary distribution of the Markov chain induced by the transition matrix of G .

Others. The *generalized topological overlap matrix* (GTOM) (Yip and Horvath 2007) of e simply measures the amount of common direct successors that the start and end nodes of e share, i.e., $C_{\text{GTOM}}(e) = \frac{|N^+(u) \cap N^+(v)| + 1}{\min\{|N^+(u)|, |N^+(v)|\}}$. The *current-flow centrality* (CFC) (Brandes and Fleischer 2005) leverages the number of flows between any two nodes $s, t \in V$ that pass through e as its centrality.

Table 1 summarizes the properties and computational complexities of the above 12 edge centrality metrics. Note that only three existing edge centrality measures, i.e., EP, EK, and EE, can be applied to directed edges and achieve a linear asymptotic performance. By (Chapela et al. 2015), $C_{\text{EP}}(e)$ and $C_{\text{EK}}(e)$ are essentially reweighted PageRank $PR(u)$ and Katz index $KA(u)$ of node u , respectively, i.e., $C_{\text{EP}}(e) = \frac{PR(u)}{|N^+(u)|}$ and $C_{\text{EK}}(e) = KA(u)$. Such a definition overlooks the topological influences from other edges on e via node v , leading to undermined edge ranking quality. EE has the same flaw as it is a special case of EK. In addition, EK produces extremely high centrality values, rendering it hard to distinguish vital edges from trivial ones. Most importantly, all these metrics rely on the strength of connections between nodes and require G to be connected, and hence, fail on disconnected networks, as exemplified in Fig. 1.

3 The ECHO Measure

In this section, we first elaborate on the design of ECHO, followed by the interpretations of ECHO, algorithmic details

for computing ECHO, and related theoretical analysis.

3.1 Optimization Objective

Distinct from existing measures, we formulate the definition of ECHO through an optimization problem with two goals. More concretely, we represent by $\mathbf{z} \in \mathbb{R}^m$ the ECHO vector, wherein $\mathbf{z}[e_i]$ signifies the ECHO value of edge e_i . In mathematical terms, ECHO vector \mathbf{z} can be obtained by optimizing the following neighborhood-related objectives:

$$\min_{\mathbf{z} \in \mathbb{R}^m} \mathcal{L} = (1 - \alpha) \|\mathbf{z} - \mathbf{x}\|^2 + \alpha \sum_{e_i, e_j \in E, i < j} \frac{1}{2} \sum_{v \in e_i \cap e_j} \frac{(\mathbf{z}_i - \mathbf{z}_j)^2}{|N^+(v)|}, \quad (2)$$

where $\forall e_i \in E$

$$\mathbf{x}[e_i] = \frac{1}{\sqrt{|N^+(u_i)| + |N^+(v_i)|}}, \quad (3)$$

and $\alpha \in (0, 1)$ is a weight balancing two optimization terms.

Intuitively, if the endpoints u_i, v_i of edge e_i are scarcely connected to others, deleting e_i from G is more likely to disconnect nodes u_i, v_i and the subgraphs containing them, engendering a considerable impact on the connectivity and structure of the entire graph. In other words, an edge e_i is less (resp. more) important to G if its endpoints are connected to a multitude of (resp. a small number of) nodes/edges, i.e., $|N^+(u_i)| + |N^+(v_i)|$ is large (resp. small). The first goal $\min_{\mathbf{z} \in \mathbb{R}^m} \|\mathbf{z} - \mathbf{x}\|^2$ in Eq. (2) enforces $\mathbf{z}[e_i]$ close to $\mathbf{x}[e_i] = \frac{1}{\sqrt{|N^+(u_i)| + |N^+(v_i)|}}$ in Eq. (3), which assigns a high (resp. low) importance value to e_i with a paucity of (resp. massive) neighbors.

On the other hand, the objective of ECHO in Eq. (2) additionally requires the centrality values of edges with common endpoints to be close. For example, given two edges e_i, e_j incident from the same node v , the difference between their ECHO values $(\mathbf{z}_i - \mathbf{z}_j)^2$ should be minimized. Considering that each edge has two endpoints and there are $|N^+(v)|$ edges incident from v in total, the average difference between two edges e_i, e_j can be quantified as $\frac{1}{2} \sum_{v \in e_i \cap e_j} \frac{(\mathbf{z}_i - \mathbf{z}_j)^2}{|N^+(v)|}$, leading to our second optimization goal in Eq. (2).

Theorem 1. *The optimal solution to Eq. (2) is expressed by*

$$\mathbf{z} = (1 - \alpha) \cdot \left(\mathbf{I} - \alpha \cdot \frac{1}{2} \mathbf{E}^\top \mathbf{D}^{-1} \mathbf{E} \right)^{-1} \mathbf{x}. \quad (4)$$

Our theoretical analysis in Theorem 1 states the closed-form solution of ECHO vector \mathbf{z} to Eq. (2). In the succeeding section, we transform it into its equivalent mathematical definitions and interpret the definitions from three perspectives.

3.2 Interpretations of ECHO

Spectral Graph Signal Filtering On the basis of Theorem 1, we can derive the following lemma:

Lemma 2. *The optimal solution to Eq. (2) is $\mathbf{z} = \mathbf{U} \frac{1}{\mathbf{I} - \alpha^2 \mathbf{\Sigma}^2} \mathbf{U}^\top \mathbf{x}$, where matrix \mathbf{U} and diagonal matrix $\mathbf{\Sigma}$ contain the left singular vectors and singular values of $\frac{1}{\sqrt{2}} \mathbf{E} \mathbf{D}^{-\frac{1}{2}}$, respectively.*

To interpret this eigendecomposition-based definition of ECHO, we first regard $\frac{1}{\sqrt{2}} \mathbf{E} \mathbf{D}^{-\frac{1}{2}} \in \mathbb{R}^{m \times n}$ as a data matrix containing m data points with n dimensions. Thus, $\frac{1}{2} \mathbf{E}^\top \mathbf{D}^{-1} \mathbf{E}$ can represent the adjacency matrix of the complete graph \tilde{G} with m data points as nodes, in which each edge (e_i, e_j) is associated with a weight $\frac{1}{2} (\mathbf{E}^\top \mathbf{D}^{-1} \mathbf{E})[e_i, e_j]$. The graph Laplacian of \tilde{G} can be derived by $\tilde{\mathbf{L}} = \mathbf{I} - \frac{1}{2} \mathbf{E}^\top \mathbf{D}^{-1} \mathbf{E}$. Let its eigendecomposition be $\tilde{\mathbf{L}} = \tilde{\mathbf{U}} \tilde{\mathbf{\Lambda}} \tilde{\mathbf{U}}^\top$, where $\tilde{\mathbf{U}}$ contains the eigenvectors and the diagonal matrix $\tilde{\mathbf{\Lambda}}$ consists of the eigenvalues of $\tilde{\mathbf{L}}$. Recall that in graph signal processing (Ortega et al. 2018), the graph Fourier transform of a signal $\mathbf{s} \in \mathbb{R}^m$ is defined as $\tilde{\mathbf{s}} = \tilde{\mathbf{U}}^\top \mathbf{s}$ and the inverse transformation is $\mathbf{s} = \tilde{\mathbf{U}} \tilde{\mathbf{s}}$. The transform enables the formulation of operations such as filtering in the spectral domain. The filtering operation on signals \mathbf{s} with a filter $g(\cdot)$ is defined as

$$\mathbf{s}^\circ = g(\mathbf{L})\mathbf{s} = g(\tilde{\mathbf{U}} \tilde{\mathbf{\Lambda}} \tilde{\mathbf{U}}^\top) \mathbf{s} = \tilde{\mathbf{U}} g(\tilde{\mathbf{\Lambda}}) \tilde{\mathbf{U}}^\top \mathbf{s}. \quad (5)$$

Lemma 3. *Let $\mathbf{U} \mathbf{\Sigma} \mathbf{V}^\top$ be the singular value decomposition (SVD) of $\frac{1}{\sqrt{2}} \mathbf{E}^\top \mathbf{D}^{-\frac{1}{2}}$. Then, $\tilde{\mathbf{U}} = \mathbf{U}$ and $\tilde{\mathbf{\Lambda}} = \mathbf{I} - \mathbf{\Sigma}^2$.*

Using Lemma 3, we can further transform the filtered signal \mathbf{s}° in Eq. (5) into its equivalent form

$$\mathbf{s}^\circ = \mathbf{U} g(\mathbf{I} - \mathbf{\Sigma}^2) \mathbf{U}^\top \mathbf{s}.$$

By Lemma 2, if we let $\mathbf{s} = \mathbf{x}$ and $\mathbf{s}^\circ = \mathbf{z}$, the above equation implies that ECHO vector \mathbf{z} is essentially the filtered signal of \mathbf{x} with filtering function $g(x) = \frac{1}{1 - \alpha^2 + \alpha^2 x}$ on graph \tilde{G} .

Markov Random Walks Eq. (4) in Theorem 1 can be further converted into its equivalent form in Eq. (6) in Lemma 4 using the Neuman series.

Lemma 4. *The optimal solution to Eq. (2) is represented as*

$$\mathbf{z} = \mathbf{B} \mathbf{x} \text{ where } \mathbf{B} = \sum_{\ell=0}^{\infty} (1 - \alpha) \alpha^\ell \left(\frac{1}{2} \mathbf{E}^\top \mathbf{D}^{-1} \mathbf{E} \right)^\ell. \quad (6)$$

Next, we expound on the definition of ECHO in Eq. (6) using Markov random walks. First, we define the *edge-wise random walk* (ERW) over G . Given network G , a jumping probability α , a source edge $e_s = (u_s, v_s)$ and a target edge $e_t = (u_t, v_t)$, an ERW on G originating from e_s proceeds as follows: at each step, the walk either (i) terminates at the current edge $e_i = (u_i, v_i)$ with a probability of $1 - \alpha$; or (ii) with the remaining α probability, jumps to node u_j that is incident with e_i ($u_j = v_i$ when G is directed and

$u_j = u_i$ or v_i with an equal likelihood when G is undirected), and subsequently navigates to one of the out-going edges (u_j, v_j) of the current node u_j (i.e., u_i or v_i) according to the probability of $\frac{1}{|N^+(u_j)|}$.

We refer to the probability of the above walk from e_s stopping at e_t in the end as the ERW score of e_t w.r.t. e_s and denote it by $r(e_s, e_t)$. Intuitively, $r(e_s, e_t)$ quantifies the strength of *multi-hop* connections from e_s to e_t with consideration of the edge directions, which can be interpreted as the total direct and indirect influences of e_s on e_t . By its definition, it can be proved that $r(e_s, e_t) = \mathbf{B}[e_i, e_j]$ and using Lemma 4 yields the following lemma:

Lemma 5. *Let $r(e_i, e_j)$ be the ERW score of edges e_i, e_j .*

$$\mathbf{z}[e_i] = \sum_{e_j \in E} \frac{r(e_i, e_j)}{\sqrt{|N^+(u_j)| + |N^+(v_j)|}} = \sum_{e_j \in E} \frac{r(e_j, e_i)}{\sqrt{|N^+(u_j)| + |N^+(v_j)|}},$$

which ranges from $1/\max_{e_i \in E} \sqrt{|N^+(u_i)| + |N^+(v_i)|}$ to $1/\min_{e_i \in E} \sqrt{|N^+(u_i)| + |N^+(v_i)|}$.

Lemma 5 indicates that the ECHO $\mathbf{z}[e_i]$ of edge e_i , is the sum of ERW scores of all edges in G when e_i is source or target, i.e., the total influence from all edges to e_i or from e_i to all edges.

Element-wise Scaled Dominant Eigenvector According to Eq. (4), we note that $\mathbf{z} = (1 - \alpha)\mathbf{x} + \frac{\alpha}{2} \mathbf{E}^\top \mathbf{D}^{-1} \mathbf{E} \mathbf{z}$. If we define $\mathbf{\Delta}$ as an m by m diagonal matrix wherein each e_i -th diagonal entry is $\mathbf{\Delta}[e_i, e_i] = m \cdot \mathbf{x}[e_i]$. Due to the symmetric property of $\mathbf{E}^\top \mathbf{D}^{-1} \mathbf{E}$, after multiplying $\mathbf{\Delta}^{-1}$, we can rewrite the above equation as follows:

$$\mathbf{y} = (1 - \alpha) \cdot \frac{1}{m} + \frac{\alpha}{2} \mathbf{E}^\top \mathbf{D}^{-1} \mathbf{E} \mathbf{y}, \quad (7)$$

where $\mathbf{y} = \mathbf{\Delta}^{-1} \mathbf{z}$. By Lemma 5, $\|\mathbf{y}\|_1 = \frac{1}{m} \sum_{e_i, e_j \in E} r(e_i, e_j) = \frac{1}{m} \sum_{e_i \in E} \|\mathbf{B}[e_i]\|_1$.

Lemma 6. *Given any $\alpha \in (0, 1)$ and integer $\ell \geq 1$, \mathbf{B} and $(\frac{1}{2} \mathbf{E}^\top \mathbf{D}^{-1} \mathbf{E})^\ell$ are semi-positive bistochastic matrices.*

Note that by Lemma 6, \mathbf{B} is a semi-positive bistochastic matrix satisfying $\|\mathbf{B}[e_i]\|_1 = 1 \forall e_i \in E$. As such, Eq. (7) can be transformed into

$$\mathbf{y} = \mathbf{H} \mathbf{y}, \text{ where } \mathbf{H} = (1 - \alpha) \cdot \frac{1 \cdot \mathbf{1}^\top}{m} + \frac{\alpha}{2} \mathbf{E}^\top \mathbf{D}^{-1} \mathbf{E}, \quad (8)$$

implying that \mathbf{y} is an eigenvector of matrix \mathbf{H} whose corresponding eigenvalue is 1. Furthermore, notice that both $\frac{1 \cdot \mathbf{1}^\top}{m}$ and $\frac{1}{2} \mathbf{E}^\top \mathbf{D}^{-1} \mathbf{E}$ (Lemma 6) are bistochastic matrices. Hence, \mathbf{H} is a positive bistochastic matrix, which is also irreducible. By Perron–Frobenius theorem (Horn and Johnson 2012), \mathbf{H} 's largest eigenvalue (in magnitude) is then 1. As a consequence, \mathbf{y} is the *dominant eigenvector* of \mathbf{H} in Eq. (8). Given that $\mathbf{z} = \mathbf{\Delta} \mathbf{y}$, \mathbf{z} is therefore an element-wise scaled version of the dominant eigenvector of \mathbf{H} .

4 Algorithms

Since the definition of ECHO introduced in Section 3.2 demands expensive eigendecomposition ($O(mn)$ time and space), we resort to leveraging Eq. (6) and Eq. (8) for the estimation of the ECHO vector in time linear to the size of G , as delineated in Sections 4.1 and 4.2, respectively.

Algorithm 1: Simple ISM

Input: $G = (V, E)$, weight α and error threshold ϵ
Output: $\mathbf{z}'[e] \forall e \in E$

- 1 Initialize a column vector $\mathbf{x} \in \mathbb{R}^m$;
 - 2 **for** $e_i \in E$ **do** Initialize $\mathbf{x}[e_i]$ as in Eq. (3) ;
 - 3 $\mathbf{z}' \leftarrow \mathbf{x}$; $t \leftarrow \lceil \log_{\alpha} \epsilon - 1 \rceil$;
 - 4 **for** $i \leftarrow 1$ **to** t **do** Compute \mathbf{z}' according to Eq. (9) ;
 - 5 **return** $\mathbf{z}'[e] \forall e \in E$;
-

Algorithm 2: Adaptive ISM

Input: $G = (V, E)$, weight α and error threshold ϵ
Output: $\mathbf{z}'[e] \forall e \in E$

Lines 1-2 are the same as Lines 1-2 in Algo. 1;

- 3 $\gamma \leftarrow \mathbf{x}$; $\mathbf{z}' \leftarrow (1 - \alpha) \cdot \gamma$;
 - 4 **while** $\exists e_i \in E$ such that $\gamma[e_i] > \epsilon$ **do**
 - 5 Update γ according to Eq. (11);
 - 6 Increase \mathbf{z}' by $(1 - \alpha) \cdot \gamma$;
 - 7 **return** $\mathbf{z}'[e] \forall e \in E$;
-

4.1 Iterative Summation Methods

Recall that in Eq. (6), \mathbf{z} involves summing up an infinite series of matrix-vector multiplications, making exact computation infeasible. A simple and straightforward way of approximating \mathbf{z} is to calculate its truncated version with a maximum number of iterations.

Simple ISM. In Algo. 1, we display the pseudo-code of this approach, which attains an absolute error ϵ in the estimated ECHO of each edge in G with a fixed number t of iterations. Algo. 1 begins by taking as input the network G , weight α , and error threshold ϵ . Afterwards, Algo. 1 initializes a length- m column vector \mathbf{x} according to Eq. (3) (Lines 1-2). After initializing \mathbf{z}' as \mathbf{x} at Line 3, Algo. 1 starts an iterative process to update \mathbf{z}' (Line 4). Specifically, in each iteration, we compute a new \mathbf{z}' by

$$\mathbf{z}' \leftarrow (1 - \alpha) \cdot \mathbf{x} + \frac{\alpha}{2} \cdot \mathbf{E}^\top \mathbf{D}^{-1} \cdot (\mathbf{E}\mathbf{z}'). \quad (9)$$

After repeating the above step for $t = \lceil \log_{\alpha} \epsilon - 1 \rceil$ iterations, Algo. 1 finally returns $\mathbf{z}'[e] \forall e \in E$ as the approximate ECHO values of all edges in G . Theorem 7 establishes the approximation accuracy guarantees for Algo. 1.

Theorem 7. *Let $\mathbf{z}'[e] \forall e \in E$ be the output of Algo. 1. Then, for each edge $e \in E$, the following inequality holds:*

$$0 \leq \mathbf{z}[e] - \mathbf{z}'[e] \leq \epsilon. \quad (10)$$

Adaptive ISM. To achieve the accuracy assurance in Eq. (10), Algo. 1 determines the maximum number t of iterations needed solely based on α and ϵ , which is data oblivious and demands more iterations. To fill this gap, we propose to compute the truncated version of Eq. (6) in an iterative and adaptive fashion. More specifically, we maintain a residual vector γ in the iterative process such that $\mathbf{z} = \mathbf{z}' + \mathbf{B}\gamma$ holds. By repeatedly converting γ into \mathbf{z}' until the values in γ reach a certain threshold, the gap between \mathbf{z} and \mathbf{z}' is reduced to satisfy Eq. (10). Algo. 2 illustrates the pseudo-code of this adaptive approach. After initializing \mathbf{x} as in Algo.

Algorithm 3: DEV Method

Input: $G = (V, E)$, weight α and integer t
Output: $\mathbf{z}'[e] \forall e \in E$

- 1 Initialize \mathbf{y} as $\frac{\mathbf{1}}{m}$;
 - 2 **for** $i \leftarrow 1$ **to** t **do** Update \mathbf{y} according to Eq. (12) ;
 - 3 **for** $e_i \in E$ **do** Compute $\mathbf{z}'[e_i]$ as in Eq. (13) ;
 - 4 **return** $\mathbf{z}'[e] \forall e \in E$;
-

1 at Lines 1-2, Algo. 2 proceeds to set the residual vector γ as \mathbf{x} and approximate ECHO vector \mathbf{z}' as $(1 - \alpha) \cdot \gamma$ (Line 3). Subsequently, if there exists any edge $e_i \in E$ such that $\gamma[e_i] > \epsilon$, we update γ by

$$\gamma \leftarrow \frac{\alpha}{2} \cdot \mathbf{E}^\top \mathbf{D}^{-1} \cdot (\mathbf{E}\gamma) \quad (11)$$

and \mathbf{z}' is then updated as $\mathbf{z}' + (1 - \alpha) \cdot \gamma$ (Lines 4-6). Otherwise, Algo. 2 ceases the above procedure and returns \mathbf{z}' as the output. As stated in Theorem 8, \mathbf{z}' is an approximate version of \mathbf{z} with at most ϵ additive error in each element.

Theorem 8. *Let $\mathbf{z}'[e] \forall e \in E$ be the output of Algo. 2. Then, for each edge $e \in E$, $0 \leq \mathbf{z}[e] - \mathbf{z}'[e] \leq \epsilon$.*

Complexity Analysis According to Algo. 1, the computation expenditure for approximate ECHO values of all edges in the input network G lies in the t iterations of matrix multiplications (Line 4). Note that $\hat{\mathbf{E}}$ and \mathbf{E} are sparse matrices containing m non-zero entries, and we can utilize the trick in Eq. (9) to reorder the sparse matrix-vector multiplications for higher efficiency. In doing so, the execution of each iteration in Line 4 takes $O(m)$ time, and thus, the time complexity for t iterations is $O\left(m \log_{\frac{1}{\alpha}} \frac{1}{\epsilon}\right)$ in total.

Suppose that Algo. 2 stops after t rounds of Lines 5-6. Then, Algo. 2 runs in $O(mt)$ time. Each iteration updates γ via Eq. (11), whose initial value is \mathbf{x} . After t iterations, $\gamma = \alpha^t \left(\frac{1}{2} \mathbf{E}^\top \mathbf{D}^{-1} \mathbf{E}\right)^t \mathbf{x}$. By Lemma 6, $\frac{1}{2} \mathbf{E}^\top \mathbf{D}^{-1} \mathbf{E}$ is bistochastic. Since Algo. 2 stops when all entries in γ are not greater than ϵ , we have $\alpha^t \max_{e_i \in E} \sum_{e_j \in E} \left(\frac{1}{2} \mathbf{E}^\top \mathbf{D}^{-1} \mathbf{E}\right)^t [e_i, e_j] \cdot \mathbf{x}[e_j] \leq \epsilon$, which leads to

$$t = \left\lceil \log_{\frac{1}{\alpha}} \max_{e_i \in E} \sum_{e_j \in E} \left(\frac{1}{2} \mathbf{E}^\top \mathbf{D}^{-1} \mathbf{E}\right)^t [e_i, e_j] \cdot \mathbf{x}[e_j] \cdot \frac{1}{\epsilon} \right\rceil \leq \left\lceil \log_{\frac{1}{\alpha}} \frac{1}{\epsilon} \right\rceil.$$

Overall, Algo. 2 takes $O\left(m \log_{\frac{1}{\alpha}} \frac{1}{\epsilon}\right)$ time in the worst case.

4.2 DEV Method

Distinct from the iterative summation methods in Section 4.1, the DEV method relies on the definition of the ECHO vector \mathbf{z} in Section 3.2. More concretely, we can first compute the dominant eigenvector \mathbf{y} of \mathbf{H} in Eq. (8). The resulting \mathbf{y} is subsequently scaled via diagonal matrix Δ , i.e., $\Delta \mathbf{y}$, to construct \mathbf{z}' . Algo. 3 presents the pseudo-code of this DEV method. Particularly, we adopt the prominent *power method* (Horn and Johnson 2012) for eigenvector computation. That is, it begins with an initial uniform vector $\frac{\mathbf{1}}{m}$ as \mathbf{y} and then computes successive t iterates $\mathbf{H}\mathbf{y}$ (Lines 1-2). The update operation $\mathbf{H}\mathbf{y}$ is implemented by

$$\mathbf{y} \leftarrow (1 - \alpha) \cdot \frac{\mathbf{1}}{m} \cdot (\mathbf{1}^\top \mathbf{y}) + \frac{\alpha}{2} \mathbf{E}^\top \mathbf{D}^{-1} \cdot (\mathbf{E}\mathbf{y}), \quad (12)$$

Table 2: Statistics of Datasets

Name	#Nodes	#Edges	#Attributes	#Classes
<i>Email-EU</i>	1,005	25,571	-	-
<i>Facebook</i>	4,039	88,234	-	-
<i>PPI</i>	3,890	76,584	-	50
<i>BlogCatalog</i>	10,312	333,983	-	39
<i>Cora</i>	2,708	10,556	1,433	7
<i>Chameleon</i>	2,277	62,792	2,325	5

whose matrix-vector multiplication orders eliminate the need for materializing $\mathbf{1} \cdot \mathbf{1}^\top$ and \mathbf{B} , thereby enabling a linear update cost for each iteration. Next, for each edge $e_i \in E$, $\mathbf{z}'[e_i]$ is calculated by

$$\mathbf{z}'[e_i] \leftarrow \frac{m}{\sqrt{|N^+(u_j)| + |N^+(v_j)|}} \cdot \mathbf{y}[e_i], \quad (13)$$

and returned as the estimation of $\mathbf{z}[e_i]$ (Lines 3-4).

Analysis According to (Wilkinson 1988), the convergence rate of the power method is given by $|\lambda_2|/|\lambda_1|$, where λ_1 and λ_2 stand for the largest and second largest eigenvalues of \mathbf{H} in terms of absolute value. Given $|\lambda_1| = 1$ as analyzed in Section 3.2, the convergence rate of Algo. 3 is $|\lambda_2|$. Note that each iteration in Line 2 involves sparse matrix multiplication in Eq. (12), which consumes $O(m)$ time. Hence, the total time cost of Algo. 3 is bounded by $O(mt)$.

5 Experiments

This section empirically studies the effectiveness of ECHO and existing edge centralities for identifying influential edges in six real-world networks through three popular graph analytics tasks, i.e., graph clustering, unsupervised network embedding, and graph neural networks, as well as their computation efficiency. Table 2 summarizes the statistics of the datasets used in the experiments. More details regarding datasets, running environments, and parameter study are deferred to our supplementary material.

We evaluate our proposed ECHO against the six best competitors, EB, ER, EP, EK, GTOM, and BDRC, out of all the edge centrality measures listed in Table 1. We exclude KPC, KEC, CFC, and IC from comparison due to their inferior ranking efficacy as well as extremely high computation overheads. Additionally, EE can be regarded as a variant of EP or EK, and thus, is omitted. Unless specified otherwise, for ECHO, we set $\alpha = 0.5$ and the maximum number of iterations to 150 (i.e., $\epsilon = 10^{-45}$ in Algo. 1). For reproducibility, all the codes and datasets are made publicly available at <https://github.com/HKBU-LAGAS/ECHO>.

5.1 Effectiveness Evaluation

In this set of experiments, we evaluate the effectiveness of ECHO and competing edge centralities as follows. After calculating the centrality values of the edges, we sort all edges of the input network G in ascending order by their centrality values. Then, we remove the top- $(m \cdot \rho)$ (ρ is varied from 0.1 to 0.9) edges from G to create a residual network G' , followed by inputting it to the classic methods, *spectral clustering* (Von Luxburg 2007), *node2vec* (Grover and Leskovec 2016), and *GCN model* (Kipf and Welling 2016) for node clustering, node classification, and semi-supervised node classification, respectively.

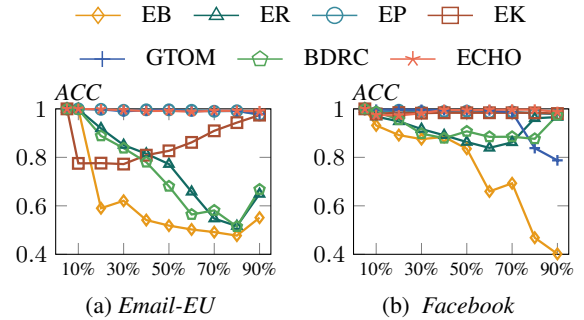


Figure 2: Node clustering accuracy via spectral clustering.

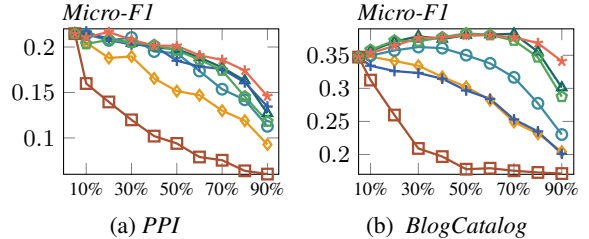


Figure 3: Node classification accuracy via node2vec.

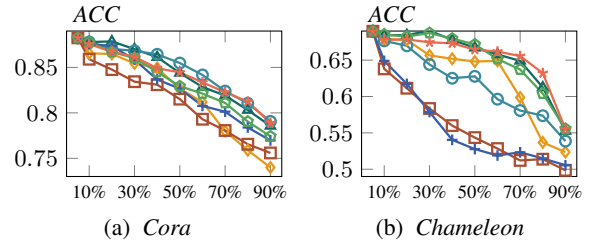


Figure 4: Node classification accuracy via GCN.

Node Clustering. First, we apply spectral clustering on the full datasets to generate the clustering results as ground-truth node labels. Fig. 2 depicts the accuracy scores achieved by all the 7 edge centrality measures on *Email-EU* and *Facebook* when varying ρ from 0.1 to 0.9 (i.e., removing 10% 90% edges from the datasets). We can observe that both EP and ECHO consistently attain the highest clustering quality on the two datasets, whereas GTOM and EK are among the best on one dataset but suffer from conspicuous performance degradation on the other one.

Node Classification with node2vec. Fig. 3 reports the micro-F1 scores for multi-label node classification by feeding the node embeddings obtained on the residual networks G' to the one-vs-rest logistic regression classifier when varying ρ from 0.1 to 0.9. From Fig. 3, we can make the following observations. First, ECHO consistently obtained the best performance on *PPI* and *BlogCatalog*. Particularly, when $\rho = 0.9$ (i.e., 90% edges are removed), ECHO is superior to all the competitors by at least 1.13% and 14% gain in micro-F1 on *PPI* and *BlogCatalog*, respectively. Second, it can be observed that EP exhibits radically different behaviors in this task, which is even inferior to BDRC and ER.

Semi-supervised Node Classification with GCN. Fig. 4, we present the semi-supervised node classification accuracy

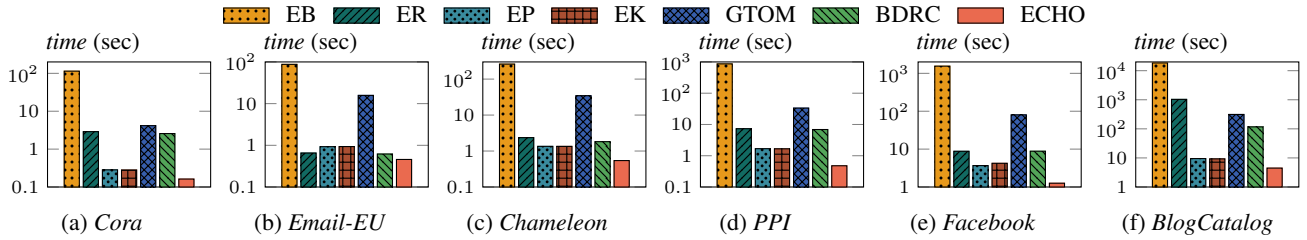


Figure 5: Computation time in seconds.

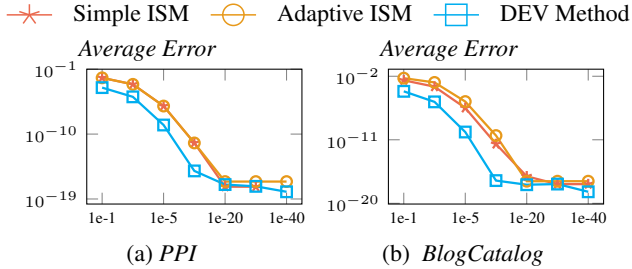


Figure 6: The convergence when varying ϵ .

scores with GCN over the residuals networks created by varying ρ from 0.1 to 0.9. on *Cora*, we can see that ECHO is second to ER and EP when $\rho \leq 70\%$. By contrast, when $\rho \geq 70\%$, ECHO is on par with the best competitor EP. Similar observation can be made on *Chameleon*, where ECHO is slightly inferior to ER and BDRC when $10\% \leq \rho \leq 50\%$ but obtains the best performance when $\rho \geq 60\%$. It’s worth noting that on *Chameleon*, EP produces a poor performance. This phenomenon reveals that EP is sensitive to both datasets and graph analytics tasks.

In summary, existing edge centrality measures either fall short of capturing network topology accurately or are sensitive to network types and structures. In comparison, ECHO achieves superior and stable performance in terms of diverse tasks on various networks, corroborating its effectiveness and robustness in the accurate identification of important and unimportant edges.

5.2 Efficiency Evaluation

In Fig. 5, we display the time costs required for the computation of ECHO and the other six centrality measures of all edges in the six tested datasets. Note that the y -axis is in log-scale, and the measurement unit for running time is a second (sec). We can observe that ECHO consistently consumes the least computation time on all datasets, whereas EB is the most expensive due to its quadratic time complexity. Compared to the most efficient existing metrics EP and EK, ECHO is $2 \times -3.49 \times$ faster on most datasets. As for ER and BDRC who are strong competitors in Fig. 3 and Fig. 4, ECHO can be up to orders of magnitude faster.

5.3 Convergence Study

In this set of experiments, we empirically study the convergence of the three algorithms in Section 4 for ECHO estimation. Let \mathbf{z} by Algo. 1 with $t = 150$ be the exact ECHO vector and \mathbf{z}' be the estimated ECHO vector. We define the *average error* of the estimation \mathbf{z}' as $\frac{1}{m} \|\mathbf{z} - \mathbf{z}'\|_1$. Fig. 6 illustrates

the average errors by the Algo. 1, Algo. 2, and Algo. 3 on representative datasets *PPI* and *BlogCatalog* when varying ϵ from 0.1 to 10^{-40} . For a fair comparison, the maximum number t of iterations in Algo. 3 is computed as Line 4 in Algo. 1. From Fig. 6, we can see that the Simple ISM and Adaptive ISM have almost identical convergence behaviors, whereas the DEV method presents conspicuously faster convergence than the iterative summation methods.

6 Other Related Work

Centrality is a major focus of network analysis, for which there exists a large body of literature, as surveyed in (Borgatti and Everett 2006; Landherr, Friedl, and Heidemann 2010; Boldi and Vigna 2014). These centrality indices are mainly designed for nodes (a.k.a. vertices). Based on the walk structures used for characterization, most of them can be classified into radial and medial centralities (Borgatti and Everett 2006). The former count walks (or trails, paths, geodesics) that start from or end at the given node, e.g., degree centrality, closeness centrality (Bavelas 1950), eigenvalue centrality (Bonacich 1972), and its variants Katz centrality (Katz 1953) and PageRank (Page et al. 1998). By contrast, the latter count walks that pass through the given node, e.g., betweenness centrality (Freeman 1977) and flow betweenness (Freeman, Borgatti, and White 1991). A similar categorization scheme for these centrality indices based on network flow is proposed in (Borgatti 2005). (Saxena and Iyengar 2020) gave a detailed discussion regarding the extensions, approximation/update algorithms, and applications of these prominent measures, as well as a brief introduction to new centrality measures proposed in recent years. (Bloch, Jackson, and Tebaldi 2023) developed a new taxonomy of these metrics based on nodal statistics and offered a list of axioms to characterize them.

7 Conclusion

In this paper, we propose a new centrality metric ECHO for ranking edges in networks. ECHO is built on our carefully crafted neighborhood-based optimization objective function, which seeks to capture the local out-degree information and ensure adjacent edges consistent in edge ranking. We conduct thorough theoretical analyses to interpret ECHO so as to facilitate an intuitive and deeper understanding of ECHO. Additionally, three linear-time algorithms with rigorous theoretical assurance are devised for the approximation of ECHO. ECHO overcomes the limitations of existing edge centrality measures in terms of both ranking effectiveness and computation efficiency. which is validated by our experiments on real-world datasets in various graph analytics tasks.

References

- Alahakoon, T.; Tripathi, R.; Kourtellis, N.; Simha, R.; and Iamnitchi, A. 2011. K-path centrality: A new centrality measure in social networks. In *Proceedings of the 4th workshop on social network systems*, 1–6.
- Altafini, D.; Bini, D. A.; Cutini, V.; Meini, B.; and Poloni, F. 2023. An edge centrality measure based on the Kemeny constant. *SIAM Journal on Matrix Analysis and Applications*, 44(2): 648–669.
- Bao, Q.; Xu, W.; and Zhang, Z. 2022. Benchmark for discriminating power of edge centrality metrics. *The Computer Journal*, 65(12): 3141–3155.
- Bavelas, A. 1950. Communication patterns in task-oriented groups. *The journal of the acoustical society of America*, 22(6): 725–730.
- Bienstock, D.; Chertkov, M.; and Harnett, S. 2014. Chance-constrained optimal power flow: Risk-aware network control under uncertainty. *Siam Review*, 56(3): 461–495.
- Bloch, F.; Jackson, M. O.; and Tebaldi, P. 2023. Centrality measures in networks. *Social Choice and Welfare*, 1–41.
- Boldi, P.; and Vigna, S. 2014. Axioms for centrality. *Internet Mathematics*, 10(3-4): 222–262.
- Bonacich, P. 1972. Factoring and weighting approaches to status scores and clique identification. *Journal of mathematical sociology*, 2(1): 113–120.
- Borgatti, S. P. 2005. Centrality and network flow. *Social networks*, 27(1): 55–71.
- Borgatti, S. P.; and Everett, M. G. 2006. A graph-theoretic perspective on centrality. *Social networks*, 28(4): 466–484.
- Brandes, U.; and Fleischer, D. 2005. Centrality measures based on current flow. In *Annual symposium on theoretical aspects of computer science*, 533–544. Springer.
- Bröhl, T.; and Lehnertz, K. 2019. Centrality-based identification of important edges in complex networks. *Chaos: An Interdisciplinary Journal of Nonlinear Science*, 29(3).
- Chapela, V.; Criado, R.; Moral, S.; and Romance, M. 2015. *Intentional risk management through complex networks analysis*. Springer.
- Crucitti, P.; Latora, V.; and Porta, S. 2006. Centrality in networks of urban streets. *Chaos: an interdisciplinary journal of nonlinear science*, 16(1).
- Cuzzocrea, A.; Papadimitriou, A.; Katsaros, D.; and Manolopoulos, Y. 2012. Edge betweenness centrality: A novel algorithm for QoS-based topology control over wireless sensor networks. *Journal of Network and Computer Applications*, 35(4): 1210–1217.
- De Meo, P.; Ferrara, E.; Fiumara, G.; and Ricciardello, A. 2012. A novel measure of edge centrality in social networks. *Knowledge-based systems*, 30: 136–150.
- Denny, N. 2020. *Bounds on the largest eigenvalue of the distance matrix of connected graphs*. Ph.D. thesis.
- Ding, L.; Steil, D.; Dixon, B.; Parrish, A.; and Brown, D. 2011. A relation context oriented approach to identify strong ties in social networks. *Knowledge-Based Systems*, 24(8): 1187–1195.
- Fey, M.; and Lenssen, J. E. 2019. Fast Graph Representation Learning with PyTorch Geometric. In *ICLR Workshop on Representation Learning on Graphs and Manifolds*.
- Fortunato, S.; Latora, V.; and Marchiori, M. 2004. Method to find community structures based on information centrality. *Physical review E*, 70(5): 056104.
- Freeman, L. C. 1977. A set of measures of centrality based on betweenness. *Sociometry*, 35–41.
- Freeman, L. C.; Borgatti, S. P.; and White, D. R. 1991. Centrality in valued graphs: A measure of betweenness based on network flow. *Social networks*, 13(2): 141–154.
- Girvan, M.; and Newman, M. E. 2002. Community structure in social and biological networks. *Proceedings of the national academy of sciences*, 99(12): 7821–7826.
- Grover, A.; and Leskovec, J. 2016. node2vec: Scalable feature learning for networks. In *Proceedings of the 22nd ACM SIGKDD*, 855–864.
- Hagberg, A.; Swart, P.; and S Chult, D. 2008. Exploring network structure, dynamics, and function using NetworkX. Technical report, Los Alamos National Lab.
- Horn, R. A.; and Johnson, C. R. 2012. *Matrix analysis*. Cambridge university press.
- Huang, X.; and Huang, W. 2019. Eigenedge: A measure of edge centrality for big graph exploration. *Journal of Computer Languages*, 55: 100925.
- Jana, D.; Malama, S.; Narasimhan, S.; and Taciroglu, E. 2023. Edge Ranking of Graphs in Transportation Networks using a Graph Neural Network (GNN). *arXiv preprint arXiv:2303.17485*.
- Katz, L. 1953. A new status index derived from sociometric analysis. *Psychometrika*, 18(1): 39–43.
- Kemeny, J. G.; and Snell, J. L. 1960. Finite markov chains. *Van Nostrand, Princeton*.
- Kipf, T. N.; and Welling, M. 2016. Semi-Supervised Classification with Graph Convolutional Networks. In *International Conference on Learning Representations*.
- Kucharczuk, N.; Was, T.; and Skibski, O. 2022. PageRank for Edges: Axiomatic Characterization. In *Proceedings of the AAAI Conference on Artificial Intelligence*, volume 36, 5108–5115.
- Lai, Y.; Lin, X.; Yang, R.; and Wang, H. 2024. Efficient Topology-aware Data Augmentation for High-Degree Graph Neural Networks. In *Proceedings of the 30th ACM SIGKDD Conference on Knowledge Discovery and Data Mining*, 1463–1473.
- Landherr, A.; Friedl, B.; and Heidemann, J. 2010. A critical review of centrality measures in social networks. *Wirtschaftsinformatik*, 52: 367–382.
- Latora, V.; and Marchiori, M. 2001. Efficient behavior of small-world networks. *Physical review letters*, 87(19): 198701.
- Leskovec, J.; Kleinberg, J.; and Faloutsos, C. 2007. Graph evolution: Densification and shrinking diameters. *ACM transactions on Knowledge Discovery from Data (TKDD)*, 1(1): 2–es.

Leskovec, J.; and Krevl, A. 2014. SNAP Datasets: Stanford Large Network Dataset Collection. <http://snap.stanford.edu/data>.

Leskovec, J.; and McAuley, J. 2012. Learning to discover social circles in ego networks. *Advances in neural information processing systems*, 25.

Li, H.; and Zhang, Z. 2018. Kirchhoff index as a measure of edge centrality in weighted networks: Nearly linear time algorithms. In *Proceedings of the ACM-SIAM SODA*, 2377–2396.

Lipman, Y.; Rustamov, R. M.; and Funkhouser, T. A. 2010. Biharmonic distance. *ACM Transactions on Graphics (TOG)*, 29(3): 1–11.

Lovász, L. 1993. Random walks on graphs. *Combinatorics, Paul erdos is eighty*, 2(1-46): 4.

Mitchell, C.; Agrawal, R.; and Parker, J. 2019. The effectiveness of edge centrality measures for anomaly detection. In *IEEE International Conference on Big Data*, 5022–5027.

Murai, S.; and Yoshida, Y. 2019. Sensitivity analysis of centralities on unweighted networks. In *The world wide web conference*, 1332–1342.

Ortega, A.; Frossard, P.; Kovačević, J.; Moura, J. M.; and Vandergheynst, P. 2018. Graph signal processing: Overview, challenges, and applications. *Proceedings of the IEEE*, 106(5): 808–828.

Page, L.; Brin, S.; Motwani, R.; and Winograd, T. 1998. The pagerank citation ranking: Bring order to the web. Technical report.

Pournajar, M.; Zaiser, M.; and Moretti, P. 2022. Edge betweenness centrality as a failure predictor in network models of structurally disordered materials. *Scientific Reports*, 12(1): 11814.

Rozemberczki, B.; Allen, C.; and Sarkar, R. 2021. Multi-scale attributed node embedding. *Journal of Complex Networks*, 9(2): cnab014.

Saxena, A.; and Iyengar, S. 2020. Centrality measures in complex networks: A survey. *arXiv preprint arXiv:2011.07190*.

Spielman, D. A.; and Srivastava, N. 2008. Graph sparsification by effective resistances. In *Proceedings of the fortieth annual ACM symposium on Theory of computing*, 563–568.

Stephenson, K.; and Zelen, M. 1989. Rethinking centrality: Methods and examples. *Social networks*, 11(1): 1–37.

Strang, G. 2023. Introduction to Linear Algebra.

Teixeira, A. S.; Monteiro, P. T.; Carriço, J. A.; Ramirez, M.; and Francisco, A. P. 2013. Spanning edge betweenness. In *Workshop on mining and learning with graphs*, volume 24, 27–31.

Von Luxburg, U. 2007. A tutorial on spectral clustering. *Statistics and computing*, 17: 395–416.

Wang, H.; Yang, R.; Huang, K.; and Xiao, X. 2023. Efficient and Effective Edge-wise Graph Representation Learning. In *SIGKDD*, 2326–2336.

White, S.; and Smyth, P. 2003. Algorithms for estimating relative importance in networks. In *Proceedings of the ninth ACM SIGKDD*, 266–275.

Wilkinson, J. H. 1988. *The algebraic eigenvalue problem*. Oxford University Press, Inc.

Yang, R.; and Tang, J. 2023. Efficient Estimation of Pairwise Effective Resistance. *SIGMOD*, 1(1): 1–27.

Yang, Z.; Cohen, W.; and Salakhudinov, R. 2016. Revisiting semi-supervised learning with graph embeddings. In *International conference on machine learning*, 40–48. PMLR.

Yi, Y.; Shan, L.; Li, H.; and Zhang, Z. 2018. Biharmonic Distance Related Centrality for Edges in Weighted Networks. In *IJCAI*, 3620–3626.

Yip, A. M.; and Horvath, S. 2007. Gene network interconnectedness and the generalized topological overlap measure. *BMC bioinformatics*, 8: 1–14.

Yoon, J.; Blumer, A.; and Lee, K. 2006. An algorithm for modularity analysis of directed and weighted biological networks based on edge-betweenness centrality. *Bioinformatics*, 22(24): 3106–3108.

Zhang, S.; Yang, R.; Tang, J.; Xiao, X.; and Tang, B. 2023. Efficient Approximation Algorithms for Spanning Centrality. In *SIGKDD*, 3386–3395.

A Proofs

Proof of Theorem 1. We rewrite the second term in Eq. (2) as

$$\begin{aligned} & \sum_{e_i, e_j \in E, i < j} \frac{1}{2} \sum_{v \in e_i \cap e_j} \frac{(\mathbf{z}_i - \mathbf{z}_j)^2}{|N^+(v)|} \\ &= \frac{1}{2} \left(\sum_{e_i \in E} \mathbf{z}_i^2 + \sum_{e_j \in E} \mathbf{z}_j^2 - 2 \sum_{e_i, e_j \in E} \sum_{v \in e_i \cap e_j} \frac{\mathbf{z}_i \mathbf{z}_j}{2|N^+(v)|} \right) \\ &= \mathbf{z}^\top \mathbf{I} \mathbf{z} - \frac{1}{2} \mathbf{z}^\top \mathbf{E}^\top \mathbf{D}^{-1} \mathbf{E} \mathbf{z} = \mathbf{z}^\top \left(\mathbf{I} - \frac{1}{2} \mathbf{E}^\top \mathbf{D}^{-1} \mathbf{E} \right) \mathbf{z}. \end{aligned}$$

By setting the derivative of the objective function \mathcal{L} to 0, i.e., $\frac{\partial \mathcal{L}}{\partial \mathbf{z}} = (1 - \alpha) \cdot (\mathbf{z} - \mathbf{x}) + \alpha \cdot \left(\mathbf{I} - \frac{1}{2} \mathbf{E}^\top \mathbf{D}^{-1} \mathbf{E} \right) \mathbf{z} = 0$, we obtain

$$\begin{aligned} \mathbf{z} &= \left(\mathbf{I} + \frac{\alpha}{1 - \alpha} \cdot \left(\mathbf{I} - \frac{1}{2} \mathbf{E}^\top \mathbf{D}^{-1} \mathbf{E} \right) \right)^{-1} \mathbf{x} \\ &= (1 - \alpha) \cdot \left((1 - \alpha) \cdot \mathbf{I} + \alpha \cdot \left(\mathbf{I} - \frac{1}{2} \mathbf{E}^\top \mathbf{D}^{-1} \mathbf{E} \right) \right)^{-1} \mathbf{x} \\ &= (1 - \alpha) \cdot \left(\mathbf{I} - \alpha \cdot \frac{1}{2} \mathbf{E}^\top \mathbf{D}^{-1} \mathbf{E} \right)^{-1} \mathbf{x}. \end{aligned} \quad (14)$$

Theorem 1 is then proved. \square

Proof of Lemma 2. Let the singular value decomposition of $\frac{1}{\sqrt{2}} \mathbf{E} \mathbf{D}^{-\frac{1}{2}}$ be $\mathbf{U} \mathbf{\Sigma} \mathbf{V}^\top$. On the other hand, by the semi-unitary property of singular vectors, i.e., $\mathbf{U}^\top \mathbf{U} = \mathbf{V}^\top \mathbf{V} = \mathbf{I}$, we have

$$\begin{aligned} \left(\mathbf{I} - \frac{\alpha}{2} \mathbf{E}^\top \mathbf{D}^{-1} \mathbf{E} \right)^{-1} &= \left(\mathbf{I} - \alpha \cdot \mathbf{U} \mathbf{\Sigma} \mathbf{V}^\top \mathbf{V} \mathbf{\Sigma} \mathbf{U}^\top \right)^{-1} \\ &= \left(\mathbf{I} - \alpha \cdot \mathbf{U} \mathbf{\Sigma}^2 \mathbf{U}^\top \right)^{-1} = \left(\mathbf{U} \cdot \left(\mathbf{I} - \alpha \mathbf{\Sigma}^2 \right) \cdot \mathbf{U}^\top \right)^{-1} \\ &= \mathbf{U} \frac{1}{\mathbf{I} - \alpha \mathbf{\Sigma}^2} \mathbf{U}^\top. \end{aligned}$$

Plugging this equality into Eq. (4) finishes the proof. \square

Proof of Lemma 3. Recall that $\tilde{\mathbf{U}}$ and $\tilde{\mathbf{\Lambda}}$ are the eigenvectors and eigenvalues of $\tilde{\mathbf{L}} = \mathbf{I} - \frac{1}{2}\mathbf{E}^\top \mathbf{D}^{-1} \mathbf{E}$, i.e.,

$$\mathbf{I} - \frac{1}{2}\mathbf{E}^\top \mathbf{D}^{-1} \mathbf{E} = \tilde{\mathbf{U}} \tilde{\mathbf{\Lambda}} \tilde{\mathbf{U}}^\top.$$

Then, we get $\frac{1}{2}\mathbf{E}^\top \mathbf{D}^{-1} \mathbf{E} = \tilde{\mathbf{U}} \cdot (\mathbf{I} - \tilde{\mathbf{\Lambda}}) \cdot \tilde{\mathbf{U}}^\top$, implying that $\tilde{\mathbf{U}}$ and $\mathbf{I} - \tilde{\mathbf{\Lambda}}$ correspond to the eigenvectors and eigenvalues of $\frac{1}{2}\mathbf{E}^\top \mathbf{D}^{-1} \mathbf{E}$, respectively. Recall the singular value decomposition of $\frac{1}{\sqrt{2}}\mathbf{E}^\top \mathbf{D}^{-\frac{1}{2}}$ is $\mathbf{U} \mathbf{\Sigma} \mathbf{V}^\top$. According to (Strang 2023), \mathbf{U} and $\mathbf{\Sigma}^2$ are the eigenvectors and eigenvalues of $\frac{1}{\sqrt{2}}\mathbf{E}^\top \mathbf{D}^{-\frac{1}{2}} \cdot (\frac{1}{\sqrt{2}}\mathbf{E}^\top \mathbf{D}^{-\frac{1}{2}})^\top = \frac{1}{2}\mathbf{E}^\top \mathbf{D}^{-1} \mathbf{E}$, respectively. Accordingly, we obtain that $\tilde{\mathbf{U}} = \mathbf{U}$ and $\tilde{\mathbf{\Lambda}} = \mathbf{I} - \mathbf{\Sigma}^2$ and the lemma is proved. \square

Proof of Lemma 4. As per Lemma 4.1 in (Denny 2020), each eigenvalue λ of a matrix $\alpha \cdot \frac{1}{2}\mathbf{E}^\top \mathbf{D}^{-1} \mathbf{E}$ is bounded by

$$\begin{aligned} |\lambda| &\leq \alpha \cdot \max_{e_i \in E} \sum_{e_j \in E} \left(\frac{1}{2}\mathbf{E}^\top \mathbf{D}^{-1} \mathbf{E} \right) [e_i, e_j] \\ &= \alpha \cdot \max_{e_i \in E} \sum_{e_j \in E} \sum_{v \in e_i \cap e_j} \frac{1}{2|N^+(v)|} = \alpha < 1. \end{aligned}$$

According to (Horn and Johnson 2012), $(\mathbf{I} - \alpha \cdot \frac{1}{2}\mathbf{E}^\top \mathbf{D}^{-1} \mathbf{E})^{-1}$ exists and can be expanded as an infinite series

$$\left(\mathbf{I} - \alpha \cdot \frac{1}{2}\mathbf{E}^\top \mathbf{D}^{-1} \mathbf{E} \right)^{-1} = \sum_{\ell=0}^{\infty} \alpha^\ell \left(\frac{1}{2}\mathbf{E}^\top \mathbf{D}^{-1} \mathbf{E} \right)^\ell. \quad (15)$$

Combining Eq. (14) and Eq. (15) leads to Eq. (6). \square

Proof of Lemma 5. As per the definitions of \mathbf{E} and \mathbf{D} , we have $\frac{1}{|N^+(u_j)|} = (\mathbf{D}^{-1} \mathbf{E})[u_j, e_j]$. Hence, the probability of jumping from $e_i = (u_i, v_i)$ to $e_j = (u_j, v_j)$ via $u_j = u_i$ or $u_j = v_i$ with one step in an ERW is $\sum_{u_j \in e_i} \frac{\mathbf{E}^\top [e_i, u_j]}{\sum_{v \in V} \mathbf{E}^\top [e_i, v]} \cdot (\mathbf{D}^{-1} \mathbf{E})[u_j, e_j] = (\frac{1}{2}\mathbf{E}^\top \mathbf{D}^{-1} \mathbf{E}) [e_i, e_j]$. As such, the probability of an ERW originating from e_s visiting e_t at ℓ -th step is $\alpha^\ell (\frac{1}{2}\mathbf{E}^\top \mathbf{D}^{-1} \mathbf{E})^\ell [e_s, e_t]$. Recall that at each step, the walk terminates at its current edge with a probability of $1 - \alpha$. Then, the probability of an ERW originating from e_s ending at e_t at ℓ -th step is $(1 - \alpha) \alpha^\ell (\frac{1}{2}\mathbf{E}^\top \mathbf{D}^{-1} \mathbf{E})^\ell [e_s, e_t]$. By considering all the steps that the walk might stop at, we can obtain the ERW score $r(e_i, e_j)$ of two edges e_i, e_j as

$$r(e_i, e_j) = \sum_{\ell=0}^{\infty} (1 - \alpha) \alpha^\ell \left(\frac{1}{2}\mathbf{E}^\top \mathbf{D}^{-1} \mathbf{E} \right)^\ell [e_i, e_j] = \mathbf{B}[e_i, e_j].$$

It can be observed that $r(e_i, e_j) = r(e_j, e_i)$ since $\mathbf{E}^\top \mathbf{D}^{-1} \mathbf{E}$ is a symmetric matrix. By Eq. (6) and the above equations, we can derive that $\mathbf{z}[e_i] = \sum_{e_j \in E} \frac{r(e_i, e_j)}{\sqrt{|N^+(u_i)| + |N^+(v_i)|}}$
 $= \sum_{e_j \in E} \frac{r(e_j, e_i)}{\sqrt{|N^+(u_j)| + |N^+(v_j)|}}$. It is easy to verify that $\sum_{e_i \in E} r(e_i, e_j) = 1$. Hence, we have $\mathbf{z}[e_i] \leq \min_{e_i \in E} \frac{1}{\sqrt{|N^+(u_i)| + |N^+(v_i)|}}$ and $\mathbf{z}[e_i] \geq \max_{e_i \in E} \frac{1}{\sqrt{|N^+(u_i)| + |N^+(v_i)|}}$, which seals the proof. \square

Proof of Lemma 6. First, we prove that $\frac{1}{2}\mathbf{E}^\top \mathbf{D}^{-1} \mathbf{E}$ is a semi-positive row-stochastic matrix. Consider any edge e_i in E . We have

$$\begin{aligned} &\sum_{e_j \in E} \left(\frac{1}{2}\mathbf{E}^\top \mathbf{D}^{-1} \mathbf{E} \right) [e_i, e_j] \\ &= \sum_{e_j \in E} \sum_{v \in V} \frac{1}{2} \mathbf{E}^\top [e_i, v] \cdot (\mathbf{D}^{-1} \mathbf{E})[v, e_j] \\ &= \sum_{v \in V} \frac{1}{2} \mathbf{E}^\top [e_i, v] \sum_{e_j \in E} (\mathbf{D}^{-1} \mathbf{E})[v, e_j] = \sum_{v \in V} \frac{1}{2} \mathbf{E}^\top [e_i, v] = 1. \end{aligned}$$

Since all the m non-zero entries in $\frac{1}{2}\mathbf{E}^\top \mathbf{D}^{-1} \mathbf{E}$ are positive, $\frac{1}{2}\mathbf{E}^\top \mathbf{D}^{-1} \mathbf{E}$ is a semi-positive row-stochastic matrix. Due to its row-stochasticity, we can generalize that $(\frac{1}{2}\mathbf{E}^\top \mathbf{D}^{-1} \mathbf{E})^\ell \forall \ell \geq 1$ is also a semi-positive row-stochastic matrix. Moreover, notice that $\frac{1}{2}\mathbf{E}^\top \mathbf{D}^{-1} \mathbf{E}$ can be represented by $\frac{1}{\sqrt{2}}\mathbf{E}^\top \mathbf{D}^{-\frac{1}{2}} \cdot (\frac{1}{\sqrt{2}}\mathbf{E}^\top \mathbf{D}^{-\frac{1}{2}})^\top$, indicating that $\frac{1}{2}\mathbf{E}^\top \mathbf{D}^{-1} \mathbf{E}$ and $(\frac{1}{2}\mathbf{E}^\top \mathbf{D}^{-1} \mathbf{E})^\ell$ are symmetric, and thus, are semi-positive bistoochastic stochastic.

Let $\mathbf{B} = \sum_{\ell=0}^{\infty} (1 - \alpha) \alpha^\ell (\frac{1}{2}\mathbf{E}^\top \mathbf{D}^{-1} \mathbf{E})^\ell$. Akin to the above analysis, \mathbf{B} is also a symmetric matrix. Besides, for every e_i -th row,

$$\begin{aligned} \sum_{e_j \in E} \mathbf{B}[e_i, e_j] &= \sum_{\ell=0}^{\infty} (1 - \alpha) \alpha^\ell \sum_{e_j \in E} \left(\frac{1}{2}\mathbf{E}^\top \mathbf{D}^{-1} \mathbf{E} \right)^\ell [e_i, e_j] \\ &= \sum_{\ell=0}^{\infty} (1 - \alpha) \alpha^\ell = 1. \end{aligned}$$

We can conclude that \mathbf{B} is symmetric and row-stochastic, i.e., a semi-positive bistoochastic matrix. \square

Proof of Theorem 7. First, we denote a truncated version of $r(e_i, e)$ by $r'(e_i, e) = \sum_{\ell=0}^t (1 - \alpha) \alpha^\ell \cdot (\frac{1}{2}\mathbf{E}^\top \mathbf{D}^{-1} \mathbf{E})^\ell [e_i, e]$. By induction, it can be shown that \mathbf{z}' obtained after t iterations can be represented by $\mathbf{z}' = \mathbf{x} \sum_{\ell=0}^t \alpha^\ell \cdot (\frac{1}{2}\mathbf{E}^\top \mathbf{D}^{-1} \mathbf{E})^\ell$. Hence, we have

$$\mathbf{z}'[e] = \sum_{e_i \in E} r'(e, e_i) \cdot \mathbf{x}[e_i] = \sum_{e_i \in E} \frac{r'(e, e_i)}{\sqrt{|N^+(u_i)| + |N^+(v_i)|}}.$$

By the definition of exact ECHO in Eq. (6), we obtain

$$\begin{aligned} \mathbf{z}[e] - \mathbf{z}'[e] &= \sum_{e_i \in E} \frac{(r(e, e_i) - r'(e, e_i))}{\sqrt{|N^+(u_i)| + |N^+(v_i)|}} \\ &= \sum_{e_i \in E} \frac{\sum_{\ell=t+1}^{\infty} (1 - \alpha) \alpha^\ell \cdot (\frac{1}{2}\mathbf{E}^\top \mathbf{D}^{-1} \mathbf{E})^\ell [e, e_i]}{\sqrt{|N^+(u_i)| + |N^+(v_i)|}} \\ &\leq \frac{\sum_{\ell=t+1}^{\infty} (1 - \alpha) \alpha^\ell \sum_{e_i \in E} (\frac{1}{2}\mathbf{E}^\top \mathbf{D}^{-1} \mathbf{E})^\ell [e, e_i]}{\min_{(u_i, v_i) \in E} \sqrt{|N^+(u_i)| + |N^+(v_i)|}} \\ &= \frac{\sum_{\ell=t+1}^{\infty} (1 - \alpha) \alpha^\ell}{\min_{(u_i, v_i) \in E} \sqrt{|N^+(u_i)| + |N^+(v_i)|}}. \end{aligned}$$

B Additional Experiments

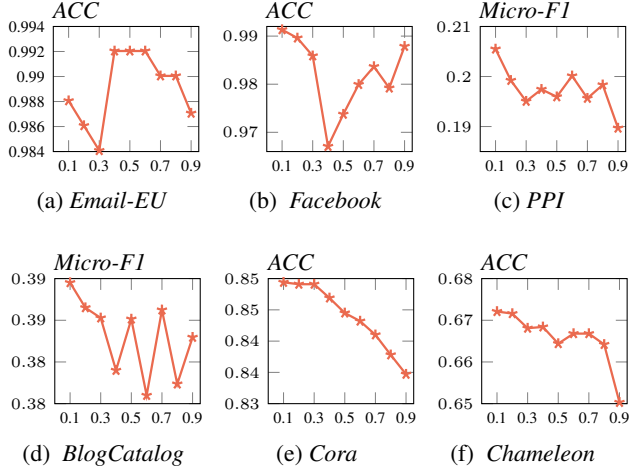


Figure 7: The performance of ECHO in downstream tasks when varying α .

Further, using the fact $\sum_{\ell=t+1}^{\infty} (1-\alpha)\alpha^{\ell} = 1 - \sum_{\ell=0}^t (1-\alpha)\alpha^{\ell} = \alpha^{t+1} = \epsilon$, we have $\mathbf{z}[e] - \mathbf{z}'[e] \leq \frac{\epsilon}{\min_{(u_i, v_i) \in E} \sqrt{|N^+(u_i)| + |N^+(v_i)|}}$. Given that u_i and v_i are two endpoints of $e_i = (u_i, v_i)$, $|N^+(u_i)| \geq 1$ and $|N^+(v_i)| \geq 0$, Eq. (10) naturally follows. \square

Proof of Theorem 8. Suppose that Algo. 2 terminates at the beginning of T -th iteration. We denote by $\gamma^{(T)}$ the vector γ at the beginning of T -th iteration. Notice that the vector $\gamma^{(T)}$ satisfies $\forall e_i \in E \gamma^{(T)}[e_i] \leq \epsilon$. According to Lines 5-6 in Algo. 2, we can derive that

$$\mathbf{z}' = \sum_{\ell=0}^{T-1} (1-\alpha)\alpha^{\ell} \left(\frac{1}{2} \mathbf{E}^{\top} \mathbf{D}^{-1} \mathbf{E} \right)^{\ell} \mathbf{x}$$

$$\gamma^{(T)} = \alpha^T \left(\frac{1}{2} \mathbf{E}^{\top} \mathbf{D}^{-1} \mathbf{E} \right)^T \mathbf{x}.$$

On this basis,

$$\begin{aligned} \mathbf{z} - \mathbf{z}' &= \sum_{\ell=T}^{\infty} (1-\alpha)\alpha^{\ell} \left(\frac{1}{2} \mathbf{E}^{\top} \mathbf{D}^{-1} \mathbf{E} \right)^{\ell} \mathbf{x} \\ &= \sum_{\ell=0}^{\infty} (1-\alpha)\alpha^{\ell} \left(\frac{1}{2} \mathbf{E}^{\top} \mathbf{D}^{-1} \mathbf{E} \right)^{\ell} \alpha^T \left(\frac{1}{2} \mathbf{E}^{\top} \mathbf{D}^{-1} \mathbf{E} \right)^T \mathbf{x} \\ &= \sum_{\ell=0}^{\infty} (1-\alpha)\alpha^{\ell} \left(\frac{1}{2} \mathbf{E}^{\top} \mathbf{D}^{-1} \mathbf{E} \right)^{\ell} \cdot \gamma^{(T)}. \end{aligned}$$

Let $\mathbf{B} = \sum_{\ell=0}^{\infty} (1-\alpha)\alpha^{\ell} \left(\frac{1}{2} \mathbf{E}^{\top} \mathbf{D}^{-1} \mathbf{E} \right)^{\ell}$ and recall that as stated in Lemma 6 \mathbf{B} is bistochastic, i.e., $\mathbf{B}\mathbf{1} = \mathbf{1}$. Then, for every edge $e_i \in E$,

$$\mathbf{z}[e_i] - \mathbf{z}'[e_i] = \sum_{e_j \in E} \mathbf{B}[e_i, e_j] \cdot \gamma^{(T)}[e_j] \leq \max_{e_j \in E} \gamma^{(T)}[e_j] \leq \epsilon,$$

which completes the proof. \square

Environment. All the experiments were conducted on a Linux machine powered by 2 Xeon Gold 6330 @2.0GHz CPUs and 1TB RAM. All the proposed methods were implemented in Python. For Edge Betweenness, we employ the NetworkX package (Hagberg, Swart, and S Chult 2008) for computation.

Datasets. We experiment with six real networks whose statistics are listed in Table 2. *Email-EU* (Leskovec, Kleinberg, and Faloutsos 2007) includes emails between members of a large research institution in Europe, whereas the *Facebook* dataset (Leskovec and McAuley 2012) contains participated Facebook users and their friendships, both of which are collected from SNAP (Leskovec and Krevl 2014). As for the *PPI* and *BlogCatalog*, they are two popular datasets used in *network embedding* (NE) (Grover and Leskovec 2016). The *PPI* dataset is a subgraph of the protein-to-protein interaction network for Homo Sapiens, wherein node labels are obtained from the hallmark gene sets and represent biological states. *BlogCatalog* is a network of social relationships among the bloggers on the BlogCatalog website, where node labels correspond to the interests of bloggers. Moreover, we include two well-known benchmark datasets for *graph neural networks* (GNNs), i.e., *Cora* (Yang, Cohen, and Salakhudinov 2016) and *Chameleon* (Rozemberczki, Allen, and Sarkar 2021). We download and preprocess them using the PyTorch Geometric Library (Fey and Lenssen 2019).

B.1 Effects of α

In this set of experiments, we study the effects of jumping probability α in ECHO on the three downstream tasks when ρ is fixed as 50%. Fig. 7 plots the spectral clustering accuracies, micro-F1 scores for node classification using node2vec, and the classification accuracy performance using GCN on six datasets when α is varied from 0.1 to 0.9. As reported, on most datasets, the best clustering and classification performance is attained when $\alpha = 0.1$. The only exception is *Email-EU*, where the highest clustering quality is achieved when $\alpha = 0.5$. Recall that α stands for the weight for our second optimization objective in Eq. (2), which is also interpreted as the probability of jumping to adjacent edges in Section 3.2. Accordingly, a low α renders an ERW tends to stop at the edges in the vicinity of the source edge. The empirical results from Fig. 7 indicate that the structural information from proximal edges (direct neighbors) is more critical for node clustering and classification tasks in networks.